THE ARABIDOPSIS ATP-BINDING CASETTE PROTEIN ATMRP5/ATABCC5 IS A HIGH-AFFINITY INOSITOL HEXA*KIS*PHOSPHATE TRANSPORTER INVOLVED IN GUARD CELL SIGNALING AND PHYTATE STORAGE

The following supplementary material is available online:

Experimental Procedures

Real time PCR- Total RNA was extracted from frozen plant material using an RNeasy plant mini kit, incorporating an RNAse-free DNAse step (Qiagen). 1µg of RNA, quantified with a NanoDrop 1000 (Thermo Scientific), was used for cDNA synthesis using random hexamer primers and Superscript II reverse transcriptase (Invitrogen, UK). Real-time PCR was performed with non-inventoried small scale TaqMan Gene Expression Assays, each containing a FAM dye-labelled TaqMan MGB probe and a PCR primer pair (Applied Biosystems). Each reaction of 25 µl volume contained the equivalent of 5 ng of reverse transcribed RNA, 33% TaqMan PCR Master Mix (Applied Biosystems), 200 nM each of the forward and reverse primer, and 100 nM of probe. Reactions were performed in microtiter plates in an ABI Prism 7900 Fast Real-Time PCR System (Applied Biosystems), according to the manufacturer's protocol. Standard curves were prepared for all samples in the range equivalent to 20–0.625 ng RNA. Expression levels were quantified relative to the gene *ACTIN2*. The details of the TaqMan Gene Expression Assays are shown below.
Small scale TaqMan Gene Expression Assays used for real-time PCR

Gene	AGI Number	Assay ID
ACTIN2	At3G18780	At02329915_s1
ITPK1	At5G16760	At02200756_g1
ITPK2	At4G08170	At02210121_g1
ITPK3	At4G33770	At02249483_g1
ITPK4	At2G43980	At02173051_g1
IPK1	At5G42810	At02314554_g1

Note, the gene names for ITPKs are those designated at the tair website http://www.arabidopsis.org/news/news.jsp. We have previously (1) *FEBS lett* 581: 4165-4171. designated ITPK2, At4G33770; and ITPK3, At4G08170.

Site-directed mutagenesis-Single amino acid exchanges in conserved domains of AtMRP5 (Fig S5A) were generated using the QuikChange®Multi Site-Directed Mutagenesis Kit (Stratagene) using the following primers bearing mismatching bases (in bold characters):
For NBD1:
Walker A_MRP5KA1: GGC ACA GTT GGC TCT GGA **GCA** TCA AGT TTT ATC TCT TGC
Walker B_MRP5DA1: GCT GAC ATT TAT TTA CTA **GCC** GAC CCT TTT AGT GCT C
ABC signature_MRP5RA1: CAG CGT GTA CAA CTT GCA **GCG** GCA TTA TAT CAA GAT GC
For NBD2:
Walker A_MRP5KA2: GGG CGA ACG GGA AGC GGA **GCG** TCG ACT TTG ATT CAA GCT
Walker B_MRP5DA2: GCC AAA ATA CTT GTT CTT **GCT** GAA GCA ACA GCA TCGG
ABC signature_MRP5RA2: CAG CTT GTG TCA CTT GGA **GCA** GCA TTA CTG AAA CAA GCC
Plasmid DNA of individual clones was isolated and sequenced to confirm the presence of the desired mutations. Mutated AtMRP5 cDNAs were cloned into the pMDC83 vector (2). Thus, the various mutated AtMRP5 cDNAs had a C-terminal GFP tag, and the AtMRP5-GFP was driven by the CaMV35S promoter. The obtained construct pCaMV35S::AtMRP5(mutated)-GFP was used to transform *mrp5-1* mutants by the floral dipping method using *Agrobacterium* GV3101 (3). Seeds were harvested and selected on $^{1}/_{2}$MS agar plates containing 1% sucrose and 25 µg/ml Hygromycin until reaching the T3 generation. Major difficulties were encountered while performing Western blots. Probably due to a very low expression we failed detecting the GFP signal, both via localization and Western blotting. Thus, all transformants (T1, T2, T3) were analyzed at DNA and RNA level. Transcripts levels were comparable to that of the wild type. cDNAs corresponding to the mutated regions were cloned and sequenced. We can state, that at least at DNA and RNA level the

mutagenized AtMRP5 cDNAs are integrated in the plant genome. Homozygous T3 plants having single amino acid exchanges in the conserved domains were subjected to a series of physiological experiments in order to monitor how their phenotype changes as compared to *mrp5-1* and Ws-2, *i.e.* stomata aperture upon treatment with ABA, drought resistance, water loss, root length, seed InsP6 content.

Subcellular localization of AtMRP5- A 1.9 kb long AtMRP5 promoter sequence was amplified from Arabidopsis genomic DNA using the following primers: promMRP5-s 5'-CCCAAGCTTGTGGAAGAACGTAGAATTCCC-3', and promMRP5-as 5'-TCCACTAGTCATGATCGGGAAAGATTTGTG-3'. By excising the CaMV35S promoter from the pMDC83 vector (2), the amplified AtMRP5 promoter was fused to the already cloned *AtMRP5–GFP* fusion. The resulting *pAtMRP5*::AtMRP5-GFPconstruct was used to transform *mrp5-1* mutants by the floral dipping method using *Agrobacterium* GV3101 (3). Seeds were harvested and selected on $^{1}/_{2}$MS 1% sucrose containing 25 µg/ml Hygromycin until T3 was reached. Homozygous T3 plants were grown for 4 weeks in the phytotron under normal growth conditions (8h dark /16 h light cycle; 21ºC, 70% relative humidity). No GFP signal was detected in vacuoles released from protoplasts isolated from those plants. As next, the plants were subjected to 14 days drought stress (8h dark /16 h light cycle; 21ºC, 70% relative humidity, no watering). Vacuoles were released by osmotic lysis from leaf protoplasts isolated from drought stressed plants. Images were captured by laser scanning confocal microscopy (DM IRE2; Leica Microsystems) using the 63X magnification objective, and an appropriate zoom.

Legends for the supplementary figures:

Figure S1 Seed content of elements that do not significantly differ in the two independent AtMRP5 mutants as compared to their corresponding wild types. The data represent the mean of four independent measurements. Error bars correspond to the standard deviation.

Figure S2 AtMRP5 encodes for a high affinity inositol hexa*kis*phosphate transporter. A second experiment of inositol hexa*kis*phosphate uptake by microsomes isolated from yeast cells harbouring AtMRP5 was performed. Uptake velocities were measured at different inositol hexa*kis*phosphate concentrations, as indicated.

Figure S3 Expression analysis of genes of inositol polyphosphate synthesis. Real-Time PCR based expression levels of IPK1 and of four members of the inositol tris/tetra*kis*phosphate kinase family in the two AtMRP5 mutants and their corresponding wild types. Error bars indicate the SD of three independent experiments. The gene names for ITPKs are those designated at the tair website http://www.arabidopsis.org/news/news.jsp

Figure S4 Guard-cell targeted expression of AtMRP5 does not restore *mrp5-1*-type root phenotype to wild type status. Seedlings of wild type, *mrp5-1* and independent transgenic T3 lines harbouring AtMRP5 driven by the MYB60 promoter were grown on vertically oriented 1/2 MS agar plates for 10 days prior to root analysis.

Figure S5 Site-directed mutagenesis of MRP5 was undertaken to elucidate the domains which play a key role for the functionality of the transporter. (*A*) Position and type of the single amino acid exchanges undertaken in key domains of AtMRP5. T3 homozygous plants carrying *pCaMV35S*::*AtMRP5* constructs with either a D771A or a D1429A exchange in the Walker B domain of NBD1 or NBD2 exhibit *mrp5-1* type seed $InsP_6$ content (*B*), root length (*C*) drought resistance (*D*) and ABA-insensitive stomatal aperture phenotype (*E*). The experiments were repeated at least three times. Error bars represent SEM. For *B*) The "p-value" indicates the confidence of significance between wild type and the three other genotypes. For *E*) The "p-value" indicates the confidence of significance between Light- and Light+ABA treatments within the same genotype. Note, while in wild type plants the stomatal aperture is significantly reduced upon ABA treatment, in *mrp5-1*, DA1 and

DA2 the stomatal apertures are significantly increased. The aperture of *mrp5-1* mutants in the light is always smaller than that of the wild type plants (4,5), but it is still significantly larger than that of ABA treated wild type plants ($p \leq 0.01$).

Figure S6 Subcellular localization of AtMRP5. An *AtMRP5–GFP* construct under the control of the native *AtMRP5* promoter was used to transform *mrp5-1* plants. Since the GFP signal was very weak, vacuoles were released by osmotic lysis from leaf protoplasts isolated from homozygous T3 plants subjected to drought stress. To verify vacuolar localization, images were captured by laser scanning confocal microscopy with the 63X magnification objective, and an appropriate zoom. (*A*) differential interference contrast (DIC) image (*B*) fluorescence signal in green, corresponding to GFP (emission λ_{em}= 500-530nm) (*C*) chlorophyll autofluorescence signal in red (emission λ_{em}= 620-750nm) (*D*) merged images of *A*, *B* and *C*.

References

1. Sweetman, D., Stavridou, I., Johnson, S., Green, P., Caddick, S.E., and Brearley, C.A. (2007) *FEBS lett* **581**, 4165-4171
2. Curtis, M., and Grossniklaus, U. (2003) *Plant Physiol* **133**, 462-469
3. Clough, S.J., and Bent, A.F. (1998) *Plant J* **16**, 735-743
4. Klein, M., Perfus-Barbeoch, L., Frelet, A., Gaedeke, N., Reinhardt D., Mueller-Roeber, B., Martinoia, E., and Forestier, C. (2003) *Plant J* **33**, 119-129
5. Gaedeke, N., Klein, M., Kolukisaoglu,U., Forestier, C., Mueller, A., Ansorge, M., Becker, D., Mamnun, Y., Kuchler, K., Schulz, B., Mueller-Roeber, B., and Martinoia,E. (2001) *The EMBO J* **20,** 1875-1887

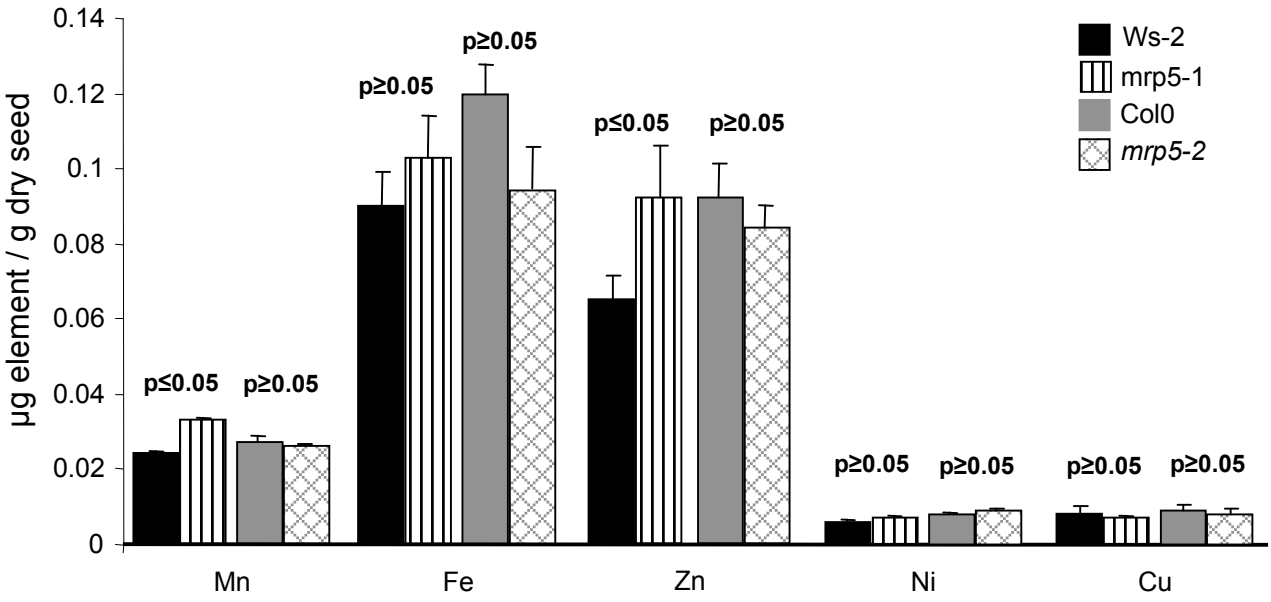
µg element / g dry seed
0.14
0.12
0.1
0.08
0.06
0.04
0.02
0
Ws-2
mrp5-1
Col0
mrp5-2
p≤0.05
p≥0.05
p≥0.05
p≥0.05
p≤0.05
p≥0.05
p≥0.05
p≥0.05
p≥0.05
p≥0.05
Mn
Fe
Zn
Ni
Cu

Figure S1

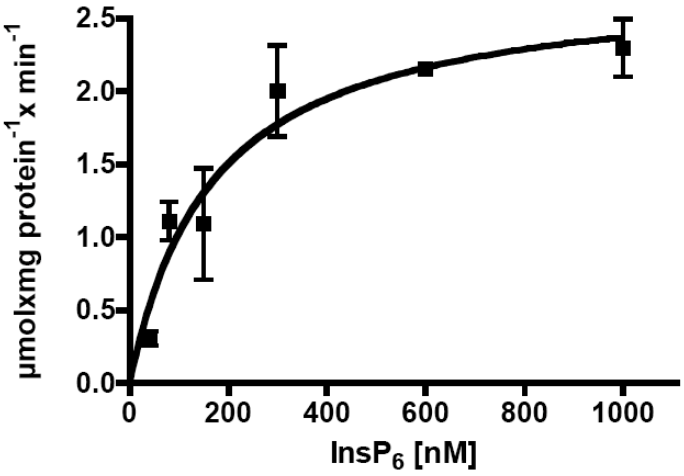
µmolxmg protein-1 x min-1
2.5
2.0
1.5
1.0
0.5
0.0
0
200
400
600
800
1000
InsP6 [nM]

Figure S2

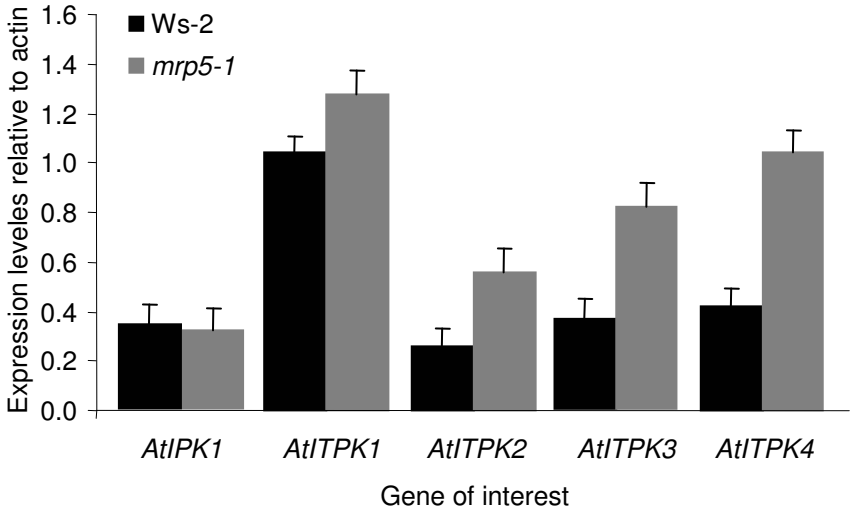
Ws-2
mrp5-1
Expression leveles relative to actin
1.6
1.4
1.2
1.0
0.8
0.6
0.4
0.2
0.0
AtIPK1
AtITPK1
AtITPK2
AtITPK3
AtITPK4
Gene of interest

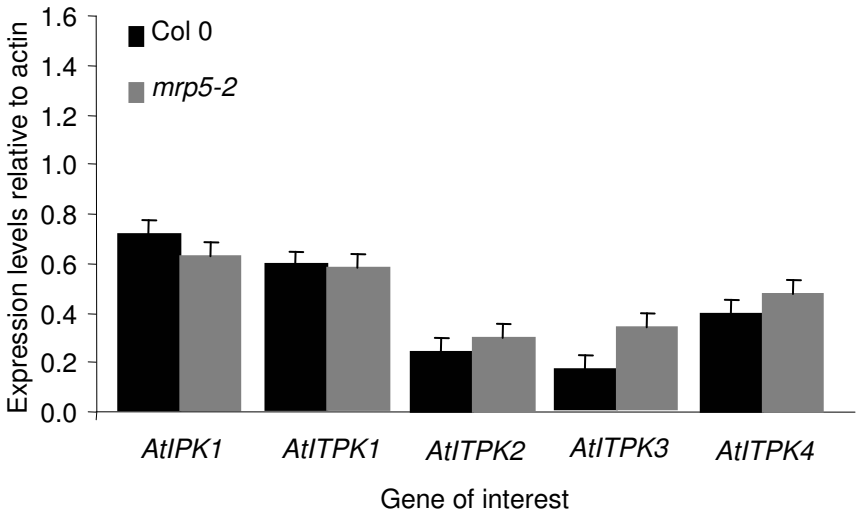
Col 0
mrp5-2
Expression levels relative to actin
1.6
1.4
1.2
1.0
0.8
0.6
0.4
0.2
0.0
AtIPK1
AtITPK1
AtITPK2
AtITPK3
AtITPK4
Gene of interest

Figure S3

A

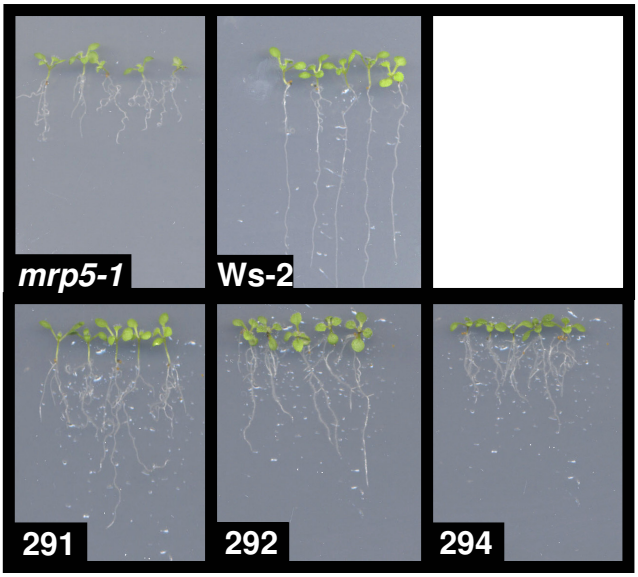

Figure S4

A

NBD1	
Walker A	K663A
Walker B	D771A (DA1)
ABC signature	R759A
NBD2	
Walker A	K1308A
Walker B	D1429A (DA2)
ABC signature	R1417A

B

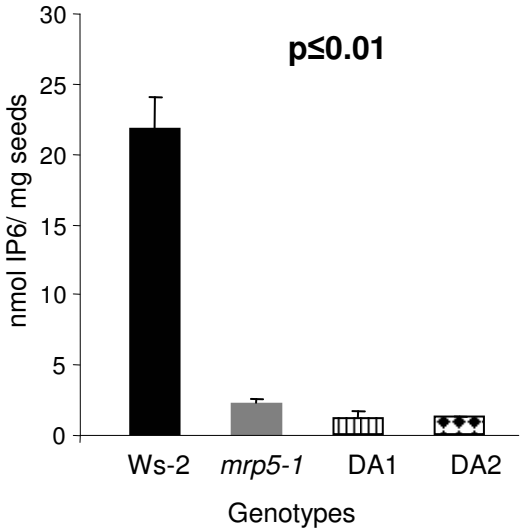

C

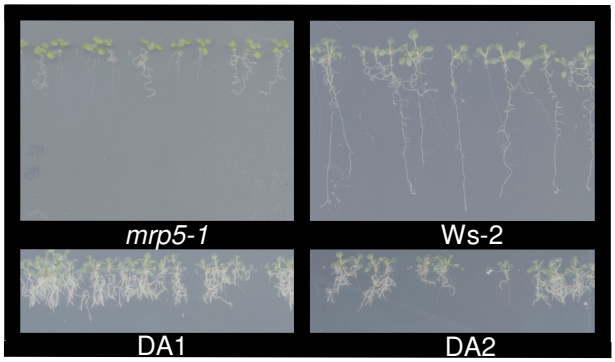

D

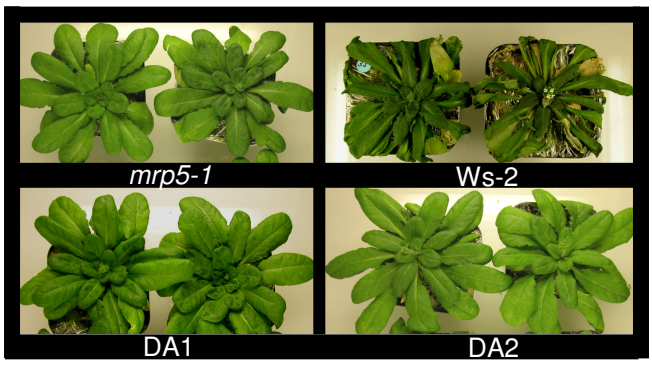

E

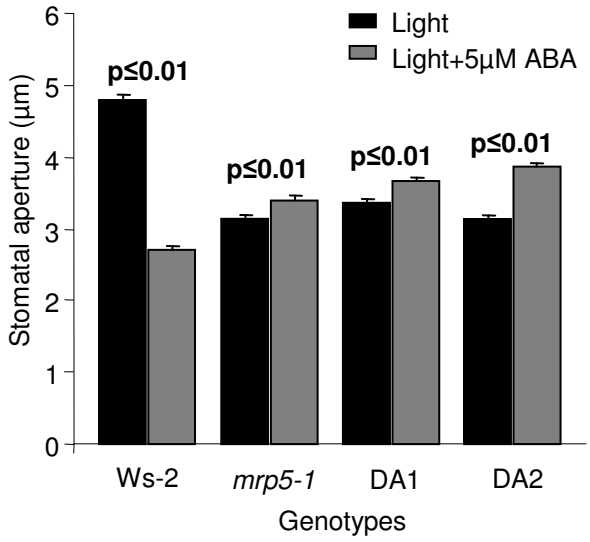

Figure S5

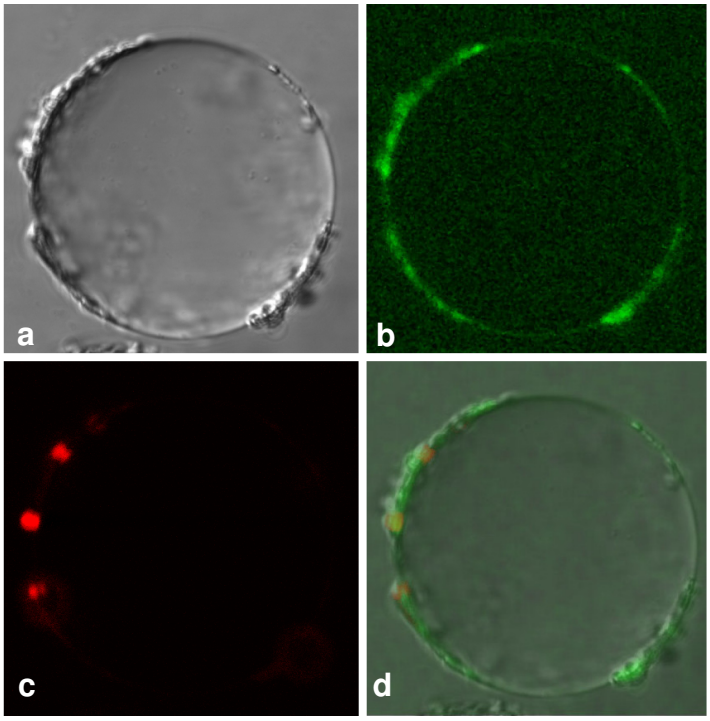

Figure S6